International Journal of Automotive Technology, Vol. 5, No. 2, pp. 77–88 (2004)

1229–9138/2004/016–02

ACTIVE DIRECT TILT CONTROL FOR STABILITY ENHANCEMENT OF A NARROW COMMUTER VEHICLE

D. PIYABONGKARN, T. KEVICZKY and R. RAJAMANI*

Department of Mechanical Engineering, University of Minnesota, 111 Church Street S.E., Minneapolis, MN 55455

(Received 5 September 2003; Revised 27 January 2004)

ABSTRACT–Narrow commuter vehicles can address many congestion, parking and pollution issues associated with urban transportation. In making narrow vehicles safe, comfortable and acceptable to the public, active tilt control systems are likely to play a crucial role. This paper focuses on the development of an active direct tilt control system for a narrow vehicle that utilizes an actuator in the vehicle suspension. A simple PD controller can stabilize the tilt dynamics of the vehicle to any desired tilt angle. However, the challenges in the tilt control system design arise in determining the desired lean angle in real-time and in minimizing tilt actuator torque requirements. Minimizing torque requirements requires the tilting and turning of the vehicle to be synchronized as closely as possible. This paper explores two different control design approaches to meet these challenges. A Receding Horizon Controller (RHC) is first developed so as to systematically incorporate preview on road curvature and synchronize tilting with driver initiated turning. Second, a nonlinear control system that utilizes feedback linearization is developed and found to be effective in reducing torque. A close analysis of the complex feedback linearization controller provides insight into which terms are important for reducing actuator effort. This is used to reduce controller complexity and obtain a simple nonlinear controller that provides good performance.

KEY WORDS : Receding horizon control, Direct tilt control, Narrow tilting vehicle, Feedback linearization

1. INTRODUCTION

The development of narrow vehicles is a promising alternative that is being proposed to address increasing traffic congestion and limited highway capacity in metropolitan areas. In order to provide an acceptable replacement for today's average passenger car, these vehicles should retain the perceived safety and the ease and comfort of driving a regular four-wheeled vehicle. Narrow vehicles currently used in urban transportation (e.g. motorcycles) require the driver to balance the vehicle while it is turning, meaning that the vehicle must be tilted into the curve to compensate for the tilting moment of the centripetal force generated by the tires. These vehicles also lack the level of safety that the majority of commuters would prefer. This could be addressed by increasing the dimensions of such a vehicle, preferably in terms of height, not to compromise the benefits gained from the narrower lane track. Building narrow vehicles taller tends to increase their tilt and the chances of a rollover during tight cornering.

Active tilt control systems that assist the driver in balancing the vehicle (and perform automatic tilting while cornering) have to be essential parts in any narrow vehicle system design that intends to provide a reasonable alternative to the current mainstream in personal transportation. The F300 Life Jet (mercedes-benz.com) for example, was developed by Daimler-Chrysler as an experimental prototype that demonstrates the feasibility of the narrow-tilting vehicle paradigm.

There are two basic types of control systems that could be used for tilting (Hibbard and Karnopp, 1993; 1996):

(1) Direct tilt control, in which an actuator is used in the vehicle suspension to control tilt.
(2) Steering tilt control (Gohl, 2003), in which the steering actuator is used to achieve the required tilt angle.

These approaches provide automatic tilting of the vehicle so the driver needs to perform only lateral control to keep the vehicle in the lane.

This paper will focus on the development of an automatic direct tilt control system for a generic narrow vehicle model that describes a prototype narrow commuter vehicle built at the Mechanical Engineering Department of the University of Minnesota. Photographs of the prototype vehicle are shown in Figure 1.

A direct tilt control (DTC) system uses an actuator in the suspension to apply a leaning torque, M_t on the vehicle. This allows the controller to tilt the vehicle to a desired angle. There are two issues that need to be addressed in a DTC system: (1) The first issue is deter-

**Corresponding author.* e-mail: rajamani@me.umn.edu

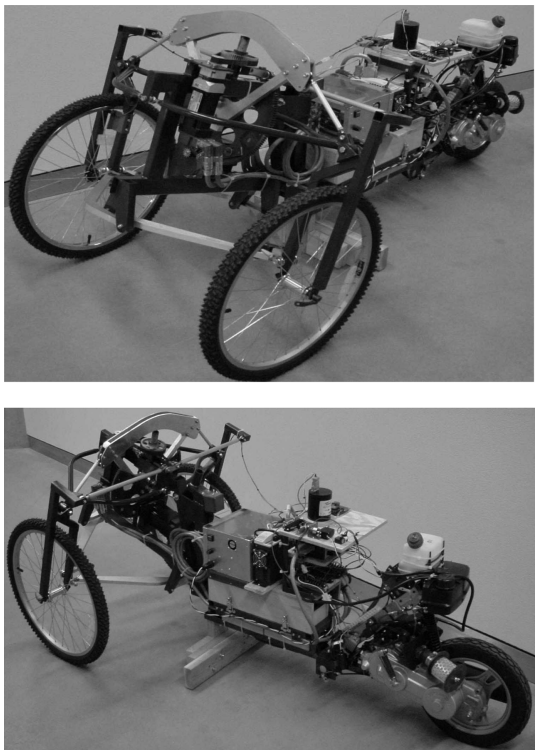

Figure 1. University of Minnesota prototype vehicle.

mining the desired lean angle of the vehicle. This may be calculated from velocity measurements and road curvature information. In real-time however, the driver's actions dictate the required lean angle for a given maneuver. Determination of the required lean angle involves interpreting the driver's intentions. (2) The second issue is reducing the torque that needs to be exerted by the actuator. We found that even though the vehicle is at an equilibrium in a perfectly coordinated turn (and hence only requires small torque for small deviations), tilting the vehicle into a turn at high speeds may require large applied torque values. The tilting and steering need to be synchronized because any lag in the tilting dynamics necessitates large peaks in the required actuator torque. The main challenge in the control design is thus to provide a systematic approach that synchronizes the tilt and cornering maneuvers in order to reduce actuator requirements and improve ride qualities.

Two different approaches are explored in the paper. First, a receding horizon controller (RHC) that makes use of preview information on the road curvature ahead of the vehicle is developed. This controller resides “on top” of two simple stabilizing controllers and initiates tilting before the actual turning begins to reduce the amount of tilting torque required when the vehicle enters the turn. Second, a nonlinear state feedback controller is developed, which provides synchronization and performance on the nonlinear vehicle model. The performance of both controllers is evaluated through extensive simulations.

2. VEHICLE MODELING

The dynamics of the vehicle can be modeled with three degrees of freedom for the vehicle's lateral position (y), yaw (ψ), and roll (θ) (Rajamani *et al.*, 2003). A schematic drawing of the vehicle with the three degrees of freedom is shown in Figure 2.

Tire slip angles with the small slip angle assumption are used to generate the lateral forces. Longitudinal dynamics are not modeled: the longitudinal velocity of the vehicle is assumed to be constant.

The nonlinear model equations obtained in (Rajamani *et al.*, 2003) are:

$$m\ddot{y}=m\dot{\psi}V+mh\ddot{\theta}\cos(\theta)-mh\dot{\theta}^2\sin(\theta)=F_f+F_r \tag{1}$$

$$I_z\ddot{\psi}=l_fF_f-l_rF_r \tag{2}$$

$$I_x\ddot{\theta}=mhg\sin(\theta)-mh^2\ddot{\theta}\sin^2(\theta)-mh^2\dot{\theta}^2\cos(\theta)\sin(\theta) -F_fh\cos(\theta)-F_rh\cos(\theta)+M_t \tag{3}$$

$$F_f=2C_f\left(\delta-\frac{\dot{y}+l_f\dot{\psi}}{V}\right)+2\lambda_f\theta \tag{4a}$$

$$F_r=C_r\left(-\frac{\dot{y}-l_r\dot{\psi}}{V}\right)+\lambda_r\theta \tag{4b}$$

The descriptions of variables and typical parameter values used are listed in Appendix A.

Define the following error coordinates (position, yaw and tilt angle errors) referenced from the center of a road

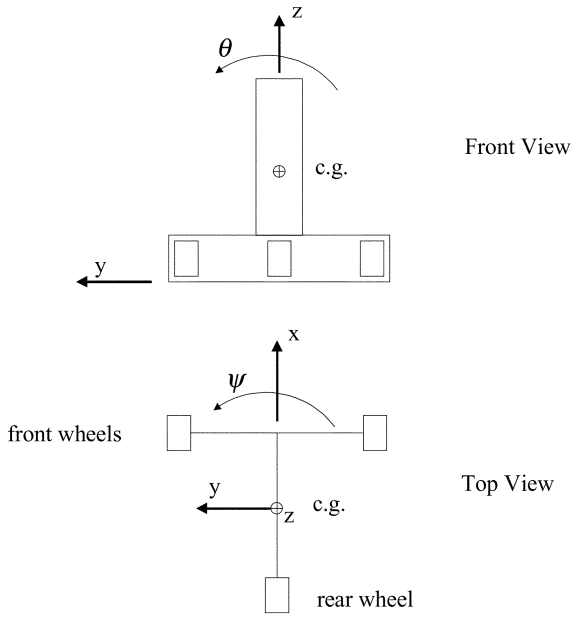

Figure 2. Vehicle degrees of freedom.

lane with a curvature of $C_V=1/R$ and with corresponding $\dot{\psi}_{des}=V/R$:

$$\ddot{e}_1=\ddot{y}+V\dot{\psi}-V\dot{\psi}_{des},\ \dot{e}_1=\dot{y}+Ve_2,\ e_1=y+V\int e_2 dt \tag{5a}$$

$$\ddot{e}_2=\ddot{\psi}-\ddot{\psi}_{des},\ \dot{e}_2=\dot{\psi}-\dot{\psi}_{des},\ e_2=\psi-\psi_{des} \tag{5b}$$

$$\ddot{e}_3=\ddot{\theta}-\ddot{\theta}_{des},\ \dot{e}_3=\dot{\theta}-\dot{\theta}_{des},\ e_3=\theta-\theta_{des} \tag{5c}$$

and the desired lean angle

$$\theta_{des}=\text{atan}\left(\frac{V^2C_V}{g}\right)=\text{atan}\left(\frac{V\dot{\psi}_{des}}{g}\right) \tag{6}$$

After linearizing about $\theta=0$, we get a state space equation of the form

$$\dot{x}=Ax+B_1\delta+B_2\dot{\psi}_{des}+B_3\theta_{des}+B_4M_t \tag{7}$$

where the state variable

$$x=[e_1\ \dot{e}_1\ e_2\ \dot{e}_2\ e_3\ \dot{e}_3]^T$$

and,

$$B_1=\begin{bmatrix}0\\ \frac{2\alpha C_f}{m}\\ 0\\ \frac{2l_fC_f}{I_z}\\ 0\\ -\frac{2hC_f}{I_x}\end{bmatrix},\quad B_2=\begin{bmatrix}0\\ -V-\frac{2\alpha C_fl_f}{mV}+\frac{\alpha C_rl_r}{mV}\\ 0\\ -\frac{2C_fl_f^2}{I_zV}+\frac{C_rl_r^2}{I_zV}\\ 0\\ -\frac{2hC_fl_f}{I_xV}+\frac{hC_rl_r}{I_xV}\end{bmatrix}$$

$$B_3=\begin{bmatrix}0\\ -\frac{mh^2g}{I_x}+\frac{\alpha\lambda_f}{m}+\frac{\alpha\lambda_r}{m}\\ 0\\ \frac{l_f\lambda_f}{I_z}-\frac{l_r\lambda_r}{I_z}\\ 0\\ -\frac{mgh}{I_x}-\frac{h\lambda_f}{I_x}-\frac{h\lambda_r}{I_x}\end{bmatrix},\ B_4=\begin{bmatrix}0\\ -\frac{h}{I_x}\\ 0\\ 0\\ 0\\ \frac{1}{I_x}\end{bmatrix},\ \alpha=1+\frac{mh^2}{I_x} \tag{8}$$

and where the matrix A is given by expression (9).

3. BASELINE CONTROL DESIGN

The objective of the automatic tilt control system to be designed is to drive all the tilt error states of the vehicle model introduced in Section 2 to zero. A driver model that acts as a state feedback controller to stabilize lateral and yaw error states is assumed. The tilt controller should also provide a systematic approach to minimize the required maximum tilting torque.

The steering angle is determined by the driver who normally follows the lane centerline. For the purpose of simulating the vehicle, the driver is modeled as a state feedback controller of the lateral and yaw error states. The steering command is therefore generated by the following (partial) state feedback law with feedback gains K_δ calculated using LQR or a pole placement technique.

$$\delta=-K_\delta x_1 \tag{10}$$

where

$$x_1=[e_1\ \ \dot{e}_1\ \ e_2\ \ \dot{e}_2]^T$$

Consider the tilt dynamics and suppose the cross coupling terms are small, we can use the LQR technique for controlling the tilt dynamic system:

$$\dot{x}_2=A_{22}x_2+B_{42}M_t \tag{11}$$

where

$$x_2=\begin{bmatrix}e_3\\ \dot{e}_3\end{bmatrix},\ A_{22}=\begin{bmatrix}A_{(55)} & A_{(56)}\\ A_{(65)} & A_{(66)}\end{bmatrix},\ B_{42}=\begin{bmatrix}B_{(45)}\\ B_{(46)}\end{bmatrix}$$

to minimize

$$J=\int_0^\infty (x_2^TQx_2+M_t^TRM_t)dt \tag{12}$$

where $Q=Q^T\geq 0, R^T>0$

The following LQR controller is then obtained

$$M_t=-K_{LQR}x_2 \tag{13}$$

where $x_2=[e_3\ \dot{e}_3]^T$

$$A=\begin{bmatrix}0 & 1 & 0 & 0 & 0 & 0\\ 0 & -\frac{2\alpha C_f}{mV}-\frac{\alpha C_r}{mV} & \frac{2\alpha C_f}{m}+\frac{\alpha C_r}{m} & -\frac{2\alpha C_fl_f}{mV}+\frac{\alpha C_rl_r}{mV} & -\frac{mgh^2}{I_x}+\frac{2\alpha\lambda_f}{m}+\frac{\alpha\lambda_r}{m} & 0\\ 0 & 0 & 0 & 1 & 0 & 0\\ 0 & -\frac{2C_fl_f}{I_zV}+\frac{C_rl_r}{I_zV} & \frac{2C_fl_f}{I_z}-\frac{C_rl_r}{I_z} & -\frac{2C_fl_f^2}{I_zV}+\frac{C_rl_r^2}{I_zV} & -\frac{2l_f\lambda_f}{I_z}-\frac{l_r\lambda_r}{I_z} & 0\\ 0 & 0 & 0 & 0 & 0 & 1\\ 0 & \frac{2hC_f}{I_xV}+\frac{hC_r}{I_xV} & -\frac{2hC_f}{I_x}-\frac{hC_r}{I_x} & -\frac{2hC_fl_f}{I_xV}+\frac{hC_rl_r}{I_xV} & \frac{mgh}{I_x}-\frac{2h\lambda_f}{I_x}-\frac{h\lambda_r}{I_x} & 0\end{bmatrix} \tag{9}$$

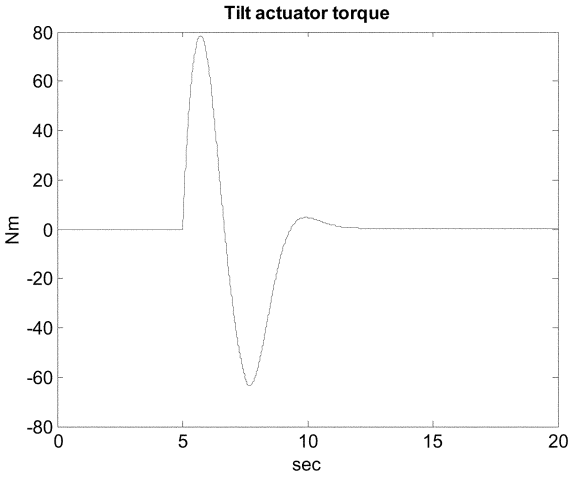

Figure 3. Control effort using baseline controller.

The LQR technique was chosen for designing both driver model and tilt controller. The weighting matrices were chosen to be $Q = I_{4\times4}$ and $R = 1$ for K_δ and $Q = I_{2\times2}$ and $R = 1$ for K_{LQR}. The LQR gains of K_δ and K_{LQR} obtained for the baseline controllers are [1 0.8524 4.1672 0.4863] and [5395.5 1393.7] respectively.

The desired tilt angle is obtained from an equation similar to equation (8):

$$\theta_{des} = \text{atan}\left(\frac{V\dot{\psi}}{g}\right)$$

and used in the implementation of the controller. $\dot{\psi}$ can be measured with a gyroscope while V can be measured with wheel speed sensors.

Figures 3-4 show the performance of the baseline controllers when the vehicle initiates a turn at 5 seconds from a straight line into a circle of radius 500 meters at a speed of 30 m/sec. As can be seen in Figure 4, the vehicle arrives at a steady state tilt angle. This steady state tilt angle is the equilibrium tilt angle for the specific turn, and results in zero lateral acceleration. During the transition from the straight road to the circular section, the vehicle begins yawing before it starts tilting. This is due to the fact that the yaw rate, measured by a gyroscope, is used to determine the desired tilt angle. As a result, the vehicle initially tilts in the wrong direction before it starts correcting itself and eventually leans towards the correct tilt angle. It requires a large tilt torque to pull the vehicle back to the steady state tilt direction. This can be seen in Figure 3 where the initial torque is as high as 80 Nm. Note that if the lateral yaw rate and tilt torque were perfectly synchronized, there would be almost no tilt torque required. Indeed, at steady state, the desired tilt angle is reached and hence the tilt torque used is zero.

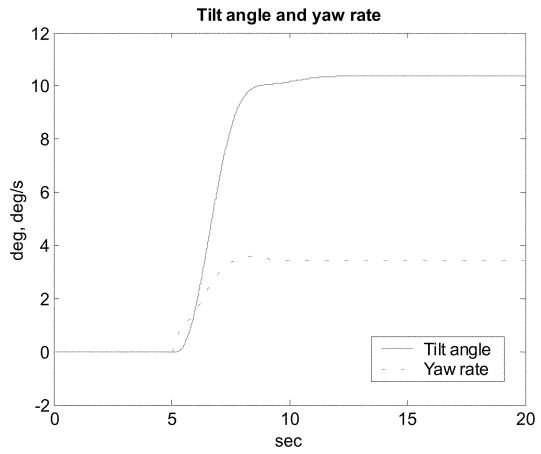

Figure 4. Tilt angle and yaw rate with baseline control.

4. RHC CONTROL DESIGN

In order to systematically reduce the required tilt torque as mentioned in Section 3, a receding horizon controller that makes use of preview information on the road curvature ahead of the vehicle was developed. Assuming that short-term preview information about the road curvature in front of the vehicle is available (e.g. provided by a lane-detection vision system or a combination of GPS tracking and road map database), the receding horizon control approach offers a systematic way of incorporating this look-ahead information into the solution of the synchronization problem. The RHC controller was designed to operate together with the two simple stabilizing baseline controllers, described in Section 3. The benefit of this control setup is the stability of the vehicle model used for prediction. Output predictions of an unstable system can be numerically very inaccurate and cause numerical problems in optimization software (Maciejowski, 2002). Hence an unstable prediction model should be avoided whenever possible. This underscores the practical importance of having a stabilizing controller augment the unstable plant before RHC methods are applied (this of course is not a theoretical necessity).

The RHC controller initiates tilting before the actual turning begins to reduce the amount of tilting torque required when the vehicle enters the turn. The rationale behind this behavior is that if the tilt controller starts acting before the front wheels start steering, then we can take advantage of the effect of gravity pulling the vehicle toward the desired lean angle. If the tilt controller waits until the vehicle has a yaw rate, then the tilting torque will have to be greatly increased to overcome the centrifugal and gravity forces.

The RHC controller has to be able to affect the torque command calculated by the LQR controller while ensuring that the tilt error e_3 would still go to zero eventually and counting on the driver's ability to provide lateral stability.

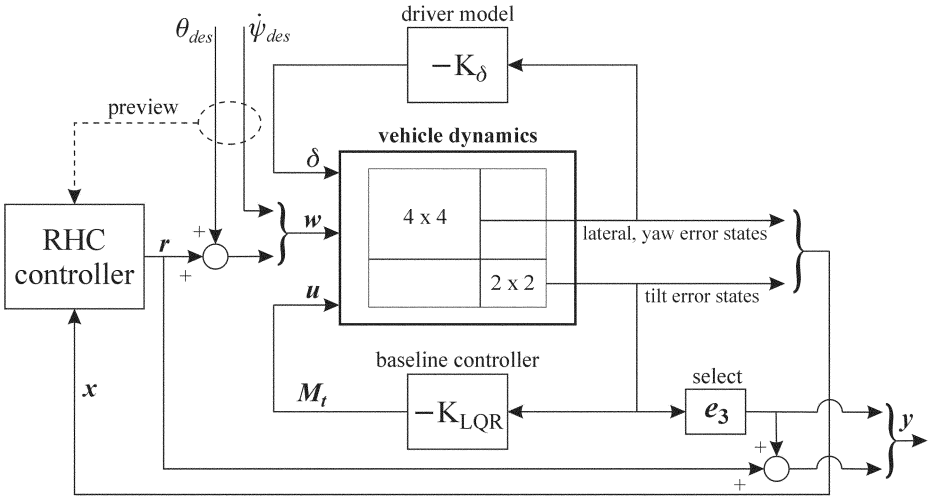

Figure 5. The proposed RHC architecture for direct tilt control.

There are several ways that an RHC controller could be designed to influence the tilt torque generated by the LQR controller. The proposed RHC setup modifies the desired tilt angle value in order to indirectly restrict the torque commands generated by the LQR controller yet retain vehicle stability and tracking of the "original" desired tilt angle that was deduced from the actual road curvature.

The proposed control architecture for using the RHC controller to modify the desired lean angle in order to affect tilting torque in an indirect way is given in Figure 5 with the following notation

$$w = [\dot{\psi}_{des} \;\; \theta_{des}]^T, r = \theta_{des\ RHC}, u = M_t \tag{14}$$

The closed-loop vehicle dynamics utilized as a prediction model in the RHC controller has the following form

$$\dot{x} = \begin{bmatrix} \overbrace{\begin{matrix} A_{11}-B_{11}K_\delta & A_{12} \\ A_{21} & A_{22}-B_{42}K_{LQR} \end{matrix}}^{A_{cl}} \end{bmatrix} + x + [\overbrace{B_2 \;\; B_3}^{B_w}]w + \overbrace{B_3}^{B_{cl}} r$$

$$\begin{bmatrix} y \\ \overline{u} \end{bmatrix} = \underbrace{\left[\begin{array}{cccccc} 0&0&0&0&1&0 \\ 0&0&0&0&1&0 \\ \hline 0&0&0&0&K_{LQR}& \end{array}\right]}_{C_{cl}} x + \underbrace{\left[\begin{array}{cc} 0&0 \\ 0&0 \\ \hline 0&0 \end{array}\right]}_{D_w} w + \underbrace{\left[\begin{array}{c} 0 \\ 1 \\ \hline 0 \end{array}\right]}_{D_{cl}} r \tag{15}$$

where the state matrices of equation (9) were partitioned according to lateral-yaw and tilt error states

$$A = \begin{bmatrix} A_{11} & A_{12} \\ A_{21} & A_{22} \end{bmatrix},$$

$$A_{11} \in \boldsymbol{R}^{4\times4}, A_{12} \in \boldsymbol{R}^{4\times2}, A_{21} \in \boldsymbol{R}^{2\times4}, A_{22} \in \boldsymbol{R}^{2\times2}$$

$$B_1 = \begin{bmatrix} B_{11} \\ B_{12} \end{bmatrix}, B_{11} \in \boldsymbol{R}^4, B_{12} \in \boldsymbol{R}^2$$

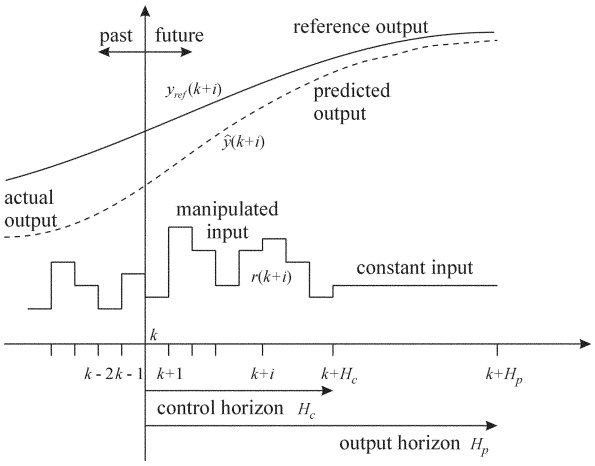

Figure 6. Receding horizon control strategy.

$$B_4 = \begin{bmatrix} B_{41} \\ B_{42} \end{bmatrix}, B_{41} \in \boldsymbol{R}^4, B_{42} \in \boldsymbol{R}^2 \tag{16}$$

The proposed control design process follows a receding horizon control approach based on a discrete-time linear time-invariant prediction model. The formulation is based on (Maciejowski, 2002).

The defining feature of RHC, or in other words model predictive control, is the repeated optimization of a performance objective over a finite prediction horizon H_p. Figure 6 characterizes the way prediction is used within the receding horizon control strategy. By manipulating the control variable r $(k+i)$ over the control horizon H_c, the algorithm drives the predicted output $\hat{y}$ $(k+i)$ over the prediction horizon towards a given reference signal y_{ref} $(k+i)$. The future control movement is determined by minimizing a performance index (cost function) subject to constraints on signals of interest. After the first control

value of the solution sequence is applied, the horizon is shifted forward in time by one time-step and the entire procedure is repeated based on the current state estimates.

The control formulation enforces actuator constraints using soft constraint formulation and ensures tracking performance. The output signals of our prediction model are assigned to these two objective groups denoted by u and y, respectively. The commanded input signals are denoted by r. For the direct tilt control problem setup, these signals are defined as

$$y = [e_3 \;\; e_3 + \theta_{des\,RHC}]^T, u = M_t, r = \theta_{des\,RHC} \tag{17}$$

The reason behind the definition of the output y is that in addition to ensuring stabilization by requiring e_3 tilt error to go to zero, we also have to make sure that the "original" steady-state desired tilt angle θ_{des} will be tracked eventually and not some other value that was modified by $\theta_{des\,RHC}$. Equation (18) clarifies this choice of a second output in view of the problem formulation that follows in the subsequent paragraphs.

$$e_3 = \theta - \theta_{desCMD} = \theta - (\theta_{des} - \theta_{desRHC}) \Rightarrow$$
$$\Rightarrow e_3 + \theta_{desRHC} = \theta - \theta_{des} \tag{18}$$

Using the notation in (17), equation (15) describes the linear vehicle model augmented with the two baseline controllers. This model was discretized with a sampling time of 0.05 sec to fit into the receding horizon control formulation used. The discrete-time closed-loop prediction model has the form

$$x(k+1) = A_{cl}x(k) + B_w w(k) + B_{cl}r(k)$$
$$\begin{bmatrix} y(k) \\ u(k) \end{bmatrix} = C_{cl}x(k) + D_w w(k) + D_{cl}r(k) \tag{19}$$

Typically, in most linear predictive controllers, the performance is specified by the following quadratic cost function to be minimized, which will also be adopted in this paper:

$$J(k) = \sum_{i=1}^{H_p} \left\| \hat{y}(k+i|k) - y_{ref}(k+i|k) \right\|_Q^2 +$$
$$+ \sum_{i=0(\delta H_c)}^{H_c-1} \left\| \Delta r(k+i|k) \right\|_Q^2 + \rho\varepsilon \tag{20}$$

where $\hat{y}(k+i|k)$ is the i-step ahead prediction of the outputs based on data up to time k. H_p denotes the output prediction horizon. These predictions of the outputs are functions of future control increments $\Delta r(k+i|k)$ for $i = 0, \delta H_c, 2\delta H_c, ..., H_c - 1$. H_c is called the control horizon, the control signal is allowed to change only at δH_c time intervals and is set to be constant for all $i \geq H_c$. The reference signal y_{ref} represents the desired outputs, Q and R are suitably chosen weighting matrices. The slack variable ε and its weight ρ is used for softening constraints. The exact purpose of the slack variable and weight in the problem formulation will be clarified shortly.

In order to obtain the predictions for the signals of interest, a model of the process is needed. By using a linear model, the resulting optimization problem of minimizing $J(k)$ will be a quadratic programming (QP) problem, for which fast and numerically reliable algorithms are available.

An alternative approach, not described in this paper, is to calculate the explicit, piecewise-affine optimal state feedback solution using multiparametric programming (Borrelli, 2003). The result of this method is a look-up table of optimal state feedback gains and values to be used based on state measurements. This approach provides the same solution as the on-line optimization based controller presented in this paper, however the online implementation requires only a function evaluation, which is attractive for applications with fast sampling time.

The linearized closed-loop vehicle model (19) is augmented with extra states to fit the formulation of the proposed online optimization based RHC scheme. Integrators are added to convert the control changes Δr into actual controls r and a simple disturbance model is incorporated to the state space description. (The disturbance model assumes constant disturbances are acting on outputs.) The constant disturbance estimates are obtained by observing the difference between measured and predicted outputs. The disturbance model also serves to mitigate the effect of model mismatch. The augmented linear closed-loop vehicle model has the following form

$$\underbrace{\begin{bmatrix} \hat{x}(k+1) \\ \hat{d}(k+1) \\ r(k) \end{bmatrix}}_{\hat{\xi}(k+1)} = \underbrace{\begin{bmatrix} A_{cl} & 0 & B_{cl} \\ 0 & I & 0 \\ 0 & 0 & I \end{bmatrix}}_{\boldsymbol{A}} \underbrace{\begin{bmatrix} \hat{x}(k) \\ \hat{d}(k) \\ r(k-1) \end{bmatrix}}_{\hat{\xi}(k)} +$$
$$\underbrace{\begin{bmatrix} B_w \\ 0 \\ 0 \end{bmatrix}}_{\boldsymbol{B}_w} w(k) + \underbrace{\begin{bmatrix} B_{cl} \\ 0 \\ I \end{bmatrix}}_{\boldsymbol{B}} \Delta r(k)$$
$$\underbrace{\begin{bmatrix} \hat{y}(k) \\ \hat{u}(k) \end{bmatrix}}_{\hat{v}(k)} = \underbrace{\left[\begin{array}{c|c|c} C_{cl} & I & D_{cl} \\ & 0 & \end{array}\right]}_{\boldsymbol{C}} \underbrace{\begin{bmatrix} \hat{x}(k) \\ \hat{d}(k) \\ r(k-1) \end{bmatrix}}_{\hat{\xi}(k)} + \underbrace{D_w}_{\boldsymbol{D}_w} w(k) + \underbrace{D}_{\boldsymbol{D}} \Delta r(k) \tag{21}$$

By using successive substitution, it is straightforward to derive that the prediction model of v outputs (signals of interest) over the prediction horizon is given by equation (22), ignoring the w input to simplify derivation.

$$\underbrace{\begin{bmatrix} \hat{v}(k+1|k) \\ \hat{v}(k+2|k) \\ \vdots \\ \hat{v}(k+H_c|k) \\ \hat{v}(k+H_c+1|k) \\ \vdots \\ \hat{v}(k+H_p|k) \end{bmatrix}}_{\boldsymbol{v}(k)} = \underbrace{\begin{bmatrix} \boldsymbol{CA} \\ \boldsymbol{CA}^2 \\ \vdots \\ \boldsymbol{CA}^{H_C} \\ \boldsymbol{CA}^{H_C+1} \\ \vdots \\ \boldsymbol{CA}^{H_p} \end{bmatrix}}_{\boldsymbol{\Psi}} \hat{\xi}(k) + \underbrace{\begin{bmatrix} \boldsymbol{CB} & \boldsymbol{D} & \cdots & 0 \\ \boldsymbol{CAB} & \boldsymbol{CB} & \boldsymbol{D} & \vdots \\ \vdots & \vdots & \ddots & \ddots \\ \boldsymbol{CA}^{H_c-1}\boldsymbol{B} & \boldsymbol{CA}^{H_c-2}\boldsymbol{B} & \cdots & \boldsymbol{CB} \\ \boldsymbol{CA}^{H_c}\boldsymbol{B} & \boldsymbol{CA}^{H_c-1}\boldsymbol{B} & \cdots & \boldsymbol{CAB} \\ \vdots & \vdots & \ddots & \ddots \\ \boldsymbol{CA}^{H_p-1}\boldsymbol{B} & \boldsymbol{CA}^{H_p-2}\boldsymbol{B} & \ldots & \boldsymbol{CA}^{H_p-H_c}\boldsymbol{B} \end{bmatrix}}_{\boldsymbol{\Theta}} \underbrace{\begin{bmatrix} \Delta r(k|k) \\ \vdots \\ \Delta r(k+H_c-1|k) \end{bmatrix}}_{\Delta \boldsymbol{R}(k)} \tag{22}$$

Having an extra input w acting on the system amounts to including an extra $\boldsymbol{\Theta}_w$ term in the above expression with the corresponding $\boldsymbol{B}_w$ and $\boldsymbol{D}_w$ matrices, if we assume that predictions are available for this input over the horizon. This term is omitted in the following to simplify the derivation. Including this term in the final result is straightforward. Leaving just the Δr inputs, consider only those predicted outputs that appear in the performance index,

$$y(k) = [\hat{y}(k+1|k), \ldots, \hat{y}(k+H_p|k)]^T,$$

$$\hat{y}(k) = \boldsymbol{C}_y \hat{\xi}(k) + \boldsymbol{D}_y \Delta r(k) \tag{23}$$

by using only the corresponding $\boldsymbol{C}_y$ and $\boldsymbol{D}_y$ matrices in expression (22). The prediction for these outputs has the form

$$y(k) = \boldsymbol{\Psi}_y \hat{\xi}(k) + \boldsymbol{\Theta}_y \Delta \boldsymbol{R}(k) \tag{24}$$

Substituting the predicted output in equation (24) into the cost function of (20), we get a quadratic expression in terms of the control changes $\Delta \boldsymbol{R}(k)$:

$$J(k) = \Delta \boldsymbol{R}(k)^T H \Delta \boldsymbol{R}(k) - \Delta \boldsymbol{R}(k)^T \boldsymbol{G} + const + \rho\varepsilon \tag{25}$$

where

$$\boldsymbol{H} = \boldsymbol{\Theta}_y^T \overline{Q} \boldsymbol{\Theta}_y + \overline{R}, \boldsymbol{G} = 2\boldsymbol{\Theta}_y^T \overline{Q} \boldsymbol{E}(k), \; const = \boldsymbol{E}^T(k) \overline{Q} \boldsymbol{E}(k) \tag{26}$$

and $\boldsymbol{E}(k)$ is defined as a tracking error between the future target trajectory and the free response of the system, i.e. $\boldsymbol{E}(k) = \boldsymbol{y}_{ref}(k) - \boldsymbol{\Psi}_y \hat{\xi}(k)$. (The only modification required in the presence of extra inputs would occur here by having an extra term in $\boldsymbol{E}(k) = \boldsymbol{y}_{ref}(k) - \boldsymbol{\Psi}_y \hat{\xi}(k) - \boldsymbol{\Theta}_w \boldsymbol{w}(k)$ based on preview information about w.) $\overline{Q}$ and $\overline{R}$ are block diagonal matrices of appropriate dimensions with Q and R on the main diagonal, respectively. Since the control objective is a regulation problem, we have $\boldsymbol{y}_{ref}(k) = 0$ for all k in the expressions of the derivation above.

As in most applications, there are level and rate limits on actuators. These are enforced as soft constraints in the problem formulation since disturbances and model mismatch can easily lead to infeasibility problems if hard constraints are enforced on these signals. Constraint softening is accomplished by introducing an additional slack variable that allows some level of constraint violation if no feasible solution exists

$$\underline{u} - \varepsilon \le \overline{u}(k+1|k), \ldots, u(k+H_p|k) \le \overline{u} + \varepsilon, \quad 0 \le \varepsilon \tag{27}$$

It is beneficial to use an ∞-norm (maximum violation) penalty on constraint violations (as shown in equation (20) and equation (27)), because it gives an exact penalty method if the weight ρ is large enough. This means that constraint violations will not occur unless no feasible solution exists to the original hard problem. If a feasible solution exists, the same solution will be obtained as with the hard formulation. Using the linear prediction model in equation (22), the constraints in equation (27) can be posed as linear constraints on the optimization variables $\Delta \boldsymbol{R}$ and ε. Finally, the QP to be solved at each time step has the following form

$$\min_{\Delta R, \varepsilon} \; \Delta \boldsymbol{R}^T H \Delta \boldsymbol{R} + \Delta \boldsymbol{R}^T \boldsymbol{G} + const + \rho\varepsilon$$

$$\text{s.t. } \boldsymbol{\Omega}_{soft} \Delta \boldsymbol{R} \le \boldsymbol{\omega}_{soft} + \varepsilon, \; 0 \le \varepsilon \tag{28}$$

5. SIMULATION RESULTS OF THE RHC APPROACH

The results of two different simulation scenarios are presented in this section to illustrate the behavior of the proposed controller. The RHC controller that was used to generate the results in this chapter relied on a realistic 1 second preview about the desired yaw rate and tilt angle that could be obtained as described in Section 4. As mentioned earlier, the prediction models were discretized with a sampling time of 0.05 sec. The horizon lengths for both simulation examples were chosen as

$$H_p = 20, \; H_c = 19, \; \delta H_c = 1$$

The vehicle was assumed to be travelling with a constant 30 m/s velocity. The RHC controller is used to follow a straight road that transitions smoothly into a

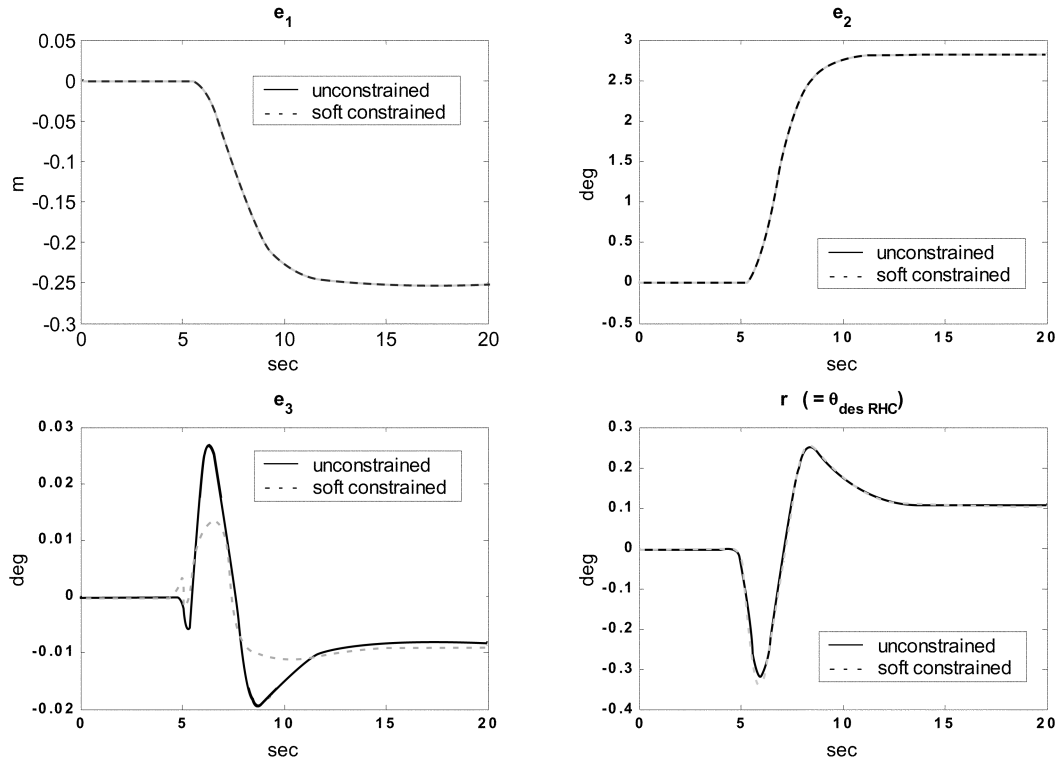

Figure 7. Lateral, yaw, and tilt error states $e_{1,2,3}$, and $\theta_{des\ RHC}$ controller output.

curve with radius of 500 m at 5 seconds into the simulation. This is represented by the corresponding changes in $\dot{\psi}_{des}$ and θ_{des}. The weighting matrices were chosen to be $Q = diag[20.\ 1]$ and $R = 0.1$. Simulations were performed with both unconstrained tilt torque actuation and with soft constraints on the tilt torque as well. In the latter case, the tilt torque was constrained to lie between -1 Nm $\leq M_t \leq$ 1 Nm. Simulation results are shown in Figures 7-9.

Figure 8 demonstrates the effectiveness of constraint enforcement. The maximum torque magnitude applied in the unconstrained case was around 2.7 Nm, whereas the use of soft constraints in the RHC setup leads to the enforcement of the desired limits and a significant reduction in the maximum applied torque. This is achieved partly by tilting the vehicle more into the turn before the actual turning happens as indicated by Figure 9. The desired "tilt-before-turn" action of the preview controller can also be observed on the tilt error signal e_3 in Figure 7.

Using soft constraints instead of hard ones, a negligible amount of constraint violation can make the problem feasible and the desired performance is retained. The coefficient ρ of the slack variable ε was selected large enough ($\rho = 10^6$) so that the violation of the constraint remains at infinitesimal levels. The mechanism to trade-off the required maximum tilting torque is again the initiation of tilting before the actual turn begins. This is

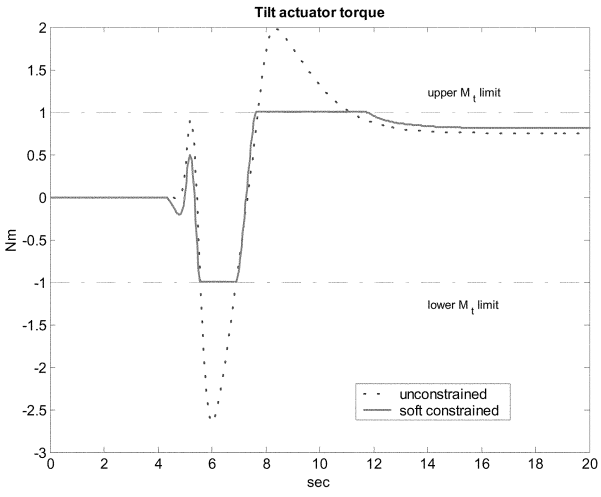

Figure 8. Tilt actuator torques M_t in the unconstrained and soft constrained cases.

accomplished by the RHC controller completely automatically, thereby constituting to a systematic procedure that provides tilt-turn synchronization. Longer preview horizons could lead to further reductions in the required maximum tilt torque. Based on simulation results, the desired tilt-turn synchronizing behavior and the overall control objectives were achieved.

The linear prediction model based RHC, however,

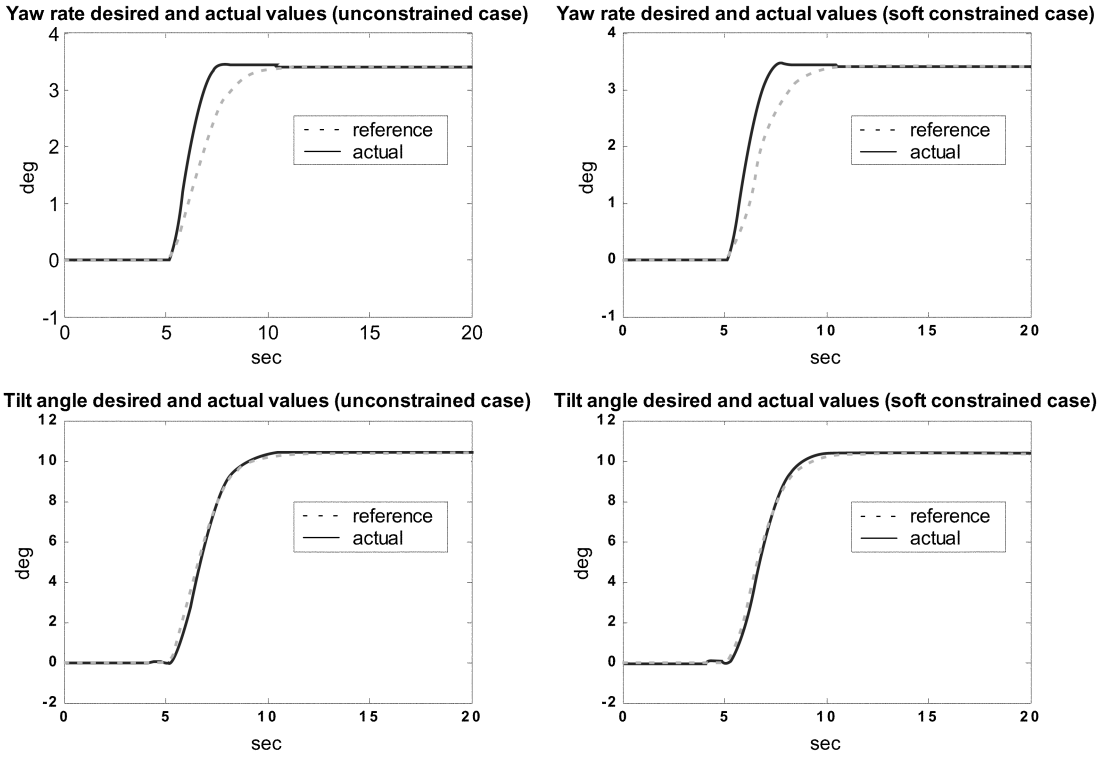

Figure 9. Yaw rates and tilt angles with their desired values.

cannot be applied directly to the nonlinear model. The model mismatch between the linearized and the nonlinear model is so significant, that the linear RHC would lead to the use of extremely large torque values, several orders of magnitude larger than in the linear model assumption. This problem could be overcome by using nonlinear predictive control methods that require a Nonlinear Program (NP) to be solved online, at each sampling time. However, besides the more complicated numerical issues that might arise, the current state-of-the-art of available computational power on a vehicle platform renders this approach infeasible in real-time.

6. NONLINEAR CONTROLLER

As described in the previous section, the linear prediction model based RHC could not be applied directly to the nonlinear model. This problem was approached using exact linearization as the basis of a nonlinear controller. The essence of the approach is to find a coordinate transformation, which performs a change of variables, and a state feedback for the nonlinear system, such that in the new coordinates and with the feedback the resulting system is linear with respect to a new input. Once we know the exact linearization of the system, we can use any of the well-established linear design techniques (even RHC) to develop a controller for the system.

We can rewrite equation (3) as

$$\ddot{\theta} = \frac{1}{I_x + mh^2\sin^2(\theta)}\{mgh\sin(\theta) - \\ -mh^2\dot{\theta}^2\cos(\theta)\sin(\theta) - (F_f + F_r)h\cos(\theta) + M_t\} \quad (29)$$

By choosing the control input M_t as

$$M_t = -mgh\sin(\theta) + mh^2\dot{\theta}^2\cos(\theta)\sin(\theta) + \\ +(F_f + F_r)h\cos(\theta) + \{I_x + mh^2\sin^2(\theta)\}u \quad (30)$$

we get

$$\ddot{\theta} = u \quad (31)$$

If u is chosen to be $u = \ddot{\theta}_d - K_D(\dot{\theta} - \ddot{\theta}_d) - K_P(\theta - \theta_d)$, we have

$$\ddot{e}_3 + K_D\dot{e}_3 + K_P e_3 = 0 \quad (32)$$

So that as long as K_P, $K_D > 0$ the system is stable.

Hence, the control input can be chosen as

$$M_t = \\ -mgh\sin(\theta) + mh^2\dot{\theta}^2\cos(\theta)\sin(\theta) + (F_f + F_r)h\cos(\theta) \\ \{I_x + mh^2\sin^2(\theta)\}\{\ddot{\theta}_d - K_D(\dot{\theta} - \dot{\theta}_d) - K_P(\theta - \theta_d)\} \quad (33)$$

This controller appears to be complex and utilizes several feedback terms. A close analysis of the feedback

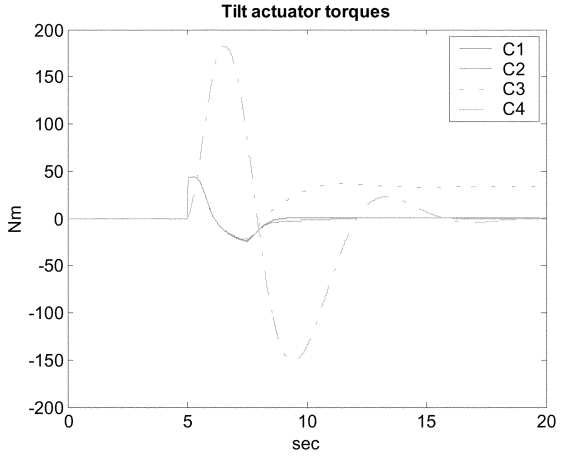

Figure 10. Comparison of actuator effort (M_t), using the four different nonlinear controller versions.

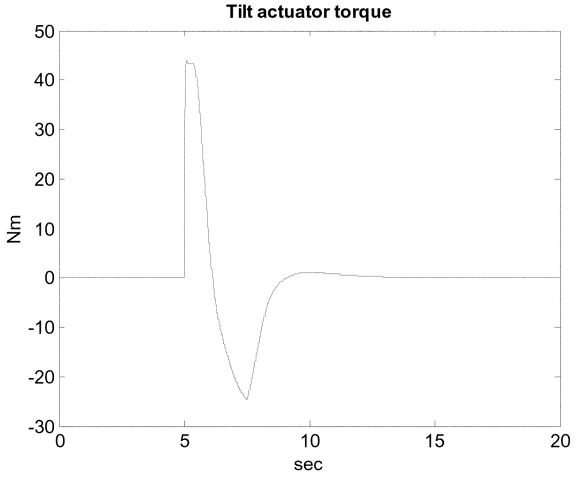

Figure 11. M_t actuator torque using nonlinear controller for r = 500 m.

linearization controller can provide insight into which terms are important for reducing actuator effort. To reduce the complexity, the effect of the various terms in equation (33) was investigated. First, the effect of the terms $mh^2\dot{\theta}^2\cos(\theta)\sin(\theta)$ and $mh^2\sin^2(\theta)$ was investigated. Ignoring these terms, equation (33) can be rewritten as

$$M_t = -mgh\sin(\theta) + (F_f + F_r)h\cos(\theta) + \\ + I_x\{\ddot{\theta}_d - K_D(\dot{\theta} - \dot{\theta}_d) - K_P(\theta - \theta_d)\} \quad (34)$$

Let M_t in equation (33) be denoted as controller C1 and in equation (34) be denoted as C2. The simulation results in Figure 10 shows that both C1 and C2 give the same performance. Hence, this means that the terms $mh^2\dot{\theta}^2\cos(\theta)\sin(\theta)$ and $mh^2\sin^2(\theta)$ are very small and can be neglected. The effect of θ and $\ddot{\theta}_d$ can be inspected by using the following controllers,

$$M_t = -mgh\theta + (F_f + F_r)h\cos(\theta) + \\ + I_x\{\ddot{\theta}_d - K_D(\dot{\theta} - \dot{\theta}_d) - K_P(\theta - \theta_d)\} \quad (35)$$

and

$$M_t = -mgh\sin(\theta) + (F_f + F_r)h\cos(\theta) + \\ + I_x\{-K_D(\dot{\theta} - \dot{\theta}_d) - K_P(\theta - \theta_d)\} \quad (36)$$

Let M_t in equation (35) be C3 and in equation (36) be C4. The simulation results in Figure 10 show that a large tilt torque is required to pull the vehicle back to the right tilt direction when using C3 and M_t is not zero at steady state when C4 is used since the desired tilt angle is not achieved. Hence, the terms $mgh\sin(\theta)$ and $I_x\ddot{\theta}_d$ in equation (33) are very important. The importance of the terms $mgh\sin(\theta)$ and $(F_f + F_r)h\cos(\theta)$ can be easily understood since these terms provide the gravity and centripetal force excitation inputs to the tilt dynamics. The term $\ddot{\theta}_d$ is a feedforward term that plays an important role in providing preview and reducing actuator effort.

Hence the final structure of the proposed controller is

$$M_t = -mgh\sin(\theta) + (F_f + F_r)h\cos(\theta) + \\ + I_x\{-K_D(\dot{\theta} - \dot{\theta}_d) - K_P(\theta - \theta_d)\} \quad (37)$$

This proposed nonlinear control law in equation (37) can be simply seen as a composition of PD terms together with important nonlinear cancellation terms. Figure 11 shows the amount of torque used by the above nonlinear controller. The tilt angle error e_3 was kept essentially zero during the entire simulation.

Figure 12 shows the performance comparison of the linear controllers (PD and LQR) and the nonlinear controller. We can see that the nonlinear controller requires the smallest amount of M_t. The linear controllers were designed using the linear model which is not accurate due to the effect of significant cross coupling steering terms and the tilt angle being away from the equilibrium point as shown in the Figure 13.

The tilt torque can be further minimized by using the following ad-hoc preview controller on top of the nonlinear control system (Gohl *et al*., 2002). The preview controller initiates tilting before the vehicle begins to turn:

IF

$$T_{curve\_begins} - T_{preview1} \le t \le T_{curve\_begins} + T_{preview2}$$

THEN

$$M_t = \frac{\alpha}{r}\mathrm{sgn}(\dot{\psi}_d) \quad (35)$$

IF

$$t \ge T_{curve\_begins} + T_{preview2}$$

THEN

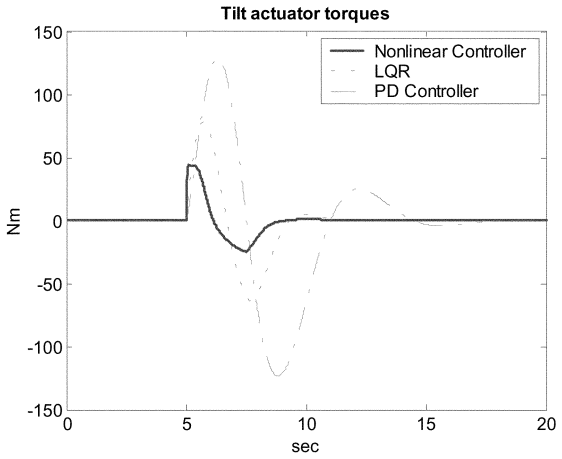

Figure 12. Performance comparison of the designed controllers comparing M_t (r = 500 m).

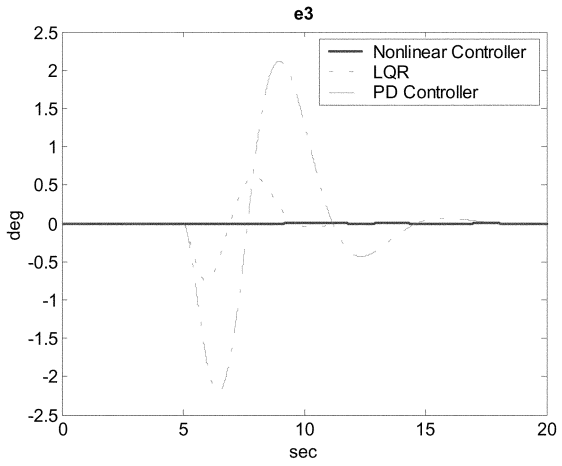

Figure 13. Performance comparison of the designed controllers comparing e_3 (r = 500 m).

$$M_t = -mgh\sin(\theta) + mh^2\dot{\theta}^2\cos(\theta)\sin(\theta) + (F_f + F_r)h\cos(\theta) + \{1 + mh^2\sin^2(\theta)\}\{\ddot{\theta}_d - K_D(\dot{\theta} - \dot{\theta}_d) - K_P(\theta - \theta_d)\} \quad (36)$$

Thus, a constant torque is output for a period of time before the vehicle actually begins turning. The magnitude of this constant torque depends on the constant and is purely a function of the preview times $T_{preview1}$ and $T_{preview2}$. For preview times equal to 0.2 and 0.6 seconds, M_t = 27 Nm was found to be appropriate in equation (35). This controller works with these parameters for other radii of the desired path and for other vehicle speeds as shown in Figures 14-15.

7. CONCLUSIONS

Active tilt control systems will play a crucial role in making narrow vehicles safe, comfortable and acceptable

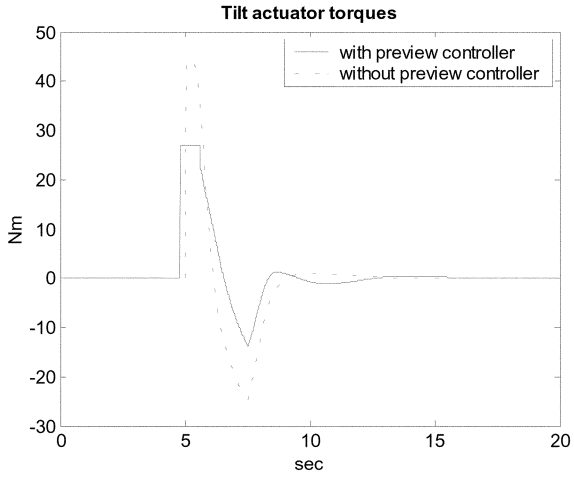

Figure 14. Tilt actuation torque with preview controller (r = 500 m).

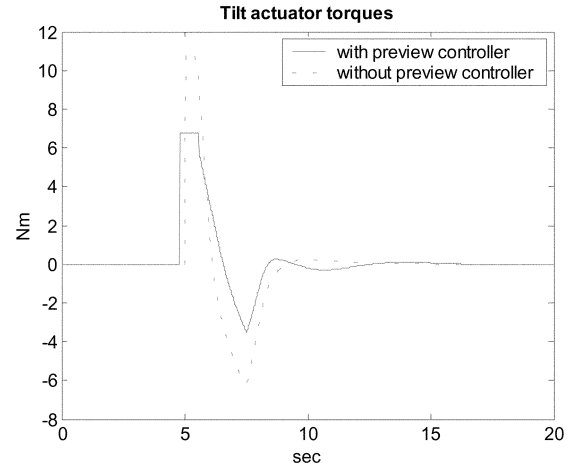

Figure 15. Tilt actuation torque with preview controller (r = 2000 m).

to the public. This paper concentrated on the development of an active direct tilt control system for a prototype narrow vehicle utilizing an actuator in the vehicle suspension. A simple PD or LQR controller could stabilize the tilt dynamics of the vehicle to any desired tilt angle. However, the challenges in the tilt control system design arose in determining the desired lean angle in real-time and in minimizing tilt actuator torque requirements. Minimizing torque requirements necessitates the tilting and turning of the vehicle to be synchronized as closely as possible. This paper explored two different approaches for the tilt control system design to achieve these goals. A Receding Horizon Controller (RHC) was first developed so as to systematically incorporate preview and synchronize tilting with driver initiated turning. Second, a nonlinear control system that utilized feedback linearization was developed and found to be effective in reducing torque. A close

analysis of the feedback linearization controller provided insight into which terms were important for reducing actuator effort. This information was used to reduce controller complexity and obtain a simple nonlinear controller that provided good performance.

ACKNOWLEDGEMENTS–This project was supported in part by a grant from the ITS Institute, University of Minnesota.

APPENDIX A: SYSTEM VARIABLES AND PARAMETERS

ψ : vehicle yaw angle
θ : vehicle tilt angle
y : lateral vehicle distance from instantaneous center of circular path
e_1 : lateral distance from a road reference ($=y - y_{des}$)
e_2 : orientation error ($=\psi - \psi_{des}$)
e_3 : tilt error ($=\theta - \theta_{des}$)
R : instantaneous radius of circular path
δ : front wheel steering angle
M_t : tilt torque from actuator
θ_{desRHC} : tilt angle command of the RHC controller
K_δ : lateral error state feedback gain (driver model)
K_{LQR} : baseline LQR tilt controller
$l_f = 0.7$ m : longitudinal distance from c.g. to front wheels
$l_r = 1.5$ m : longitudinal distance from c.g. to rear wheels
$h = 1$ m : height of c.g. of vehicle from ground
$m = 275$ kg : mass of vehicle
$I_z = 120$ kg m^2 : yaw moment of inertia of vehicle
$I_x = 180$ kg m^2 : tilting moment of inertia of vehicle
$C_f = 3500$ kg m^2/s^2 : cornering stiffness of each front wheel
$C_r = 3000$ kg m^2/s^2 : cornering stiffness of each rear wheel
$\lambda_f = 0$ N/rad : camber stiffness of each front wheel
$\lambda_r = 0$ N/rad : camber stiffness of each rear wheel
$g = 9.81$ m/s^2 : gravitational constant
$V = 30$ m/s : vehicle longitudinal speed

$$\ddot{e}_1 = \dddot{y} + V\ddot{\psi} - V\ddot{\psi}_{des}, \dot{e}_1 = \ddot{y} + V\dot{e}_2, e_1 = y + V\int e_2 dt$$

$$\ddot{e}_2 = \ddot{\psi} - \ddot{\psi}_{des}, \dot{e}_2 = \dot{\psi} - \dot{\psi}_{des}, e_2 = \psi - \psi_{des}$$

$$\dddot{e}_3 = \dddot{\theta} - \dddot{\theta}_{des}, \ddot{e}_3 = \ddot{\theta} - \ddot{\theta}_{des}, \dot{e}_3 = \dot{\theta} - \dot{\theta}_{des}, e_3 = \theta - \theta_{des}$$

$$x_1 = [e_1 \ \dot{e}_1 \ e_2 \ \ \dot{e}_2]^T, x_2 = [e_3 \ \dot{e}_3]^T$$

$\dot{\psi}_{des} = VC_V$ desired yaw rate

$$\theta_{des} = \text{atan}\left(\frac{V^2 C_V}{g}\right) = \text{atan}\left(\frac{C\dot{\psi}_{des}}{g}\right) \text{ desired tilt angle}$$

According to these definitions, $e_1 > 0$ when the vehicle is on the inside of the curve since $\dot{\psi} - \dot{\psi}_d > 0$.

REFERENCES

Borrelli, F. (2003). *Constrained Optimal Control of Linear and Hybrid Systems*. Lecture Notes in Control and Information Sciences 290. Springer-Verlag, New York.

Gohl, J. (2003). Narrow tilting vehicles: modeling, steering based tilt control. *Masters Thesis*. University of Minnesota, April.

Gohl, J., Rajamani, R., Alexander, L. and Starr, P. (2002). The development of tilt-controlled narrow ground vehicles. *Proceedings of the American Control Conference, Anchorage*, AK, May 8–10.

Hibbard, R. and Karnopp, D. (1993). The dynamics of small, relatively tall and narrow tilting ground vehicles. *ASME Publication DSC* **52**, Advanced Automotive Technologies, 397–417.

Hibbard, R. and Karnopp, D. (1996). Twenty-first century transportation system solutions a new type of small, relatively tall and narrow tilting commuter vehicle. *Vehicle System Dynamics* **25**, 321–347.

http://www.mercedes-benz.com/e/innovation/fmobil/f300_mobilitaet.htm.

Maciejowski, J. M. (2002). *Predictive Control with Constraints*, Prentice Hall. New Jersey.

Rajamani, R., Gohl, J., Alexander, L. and Starr, P. (2003). Dynamics of narrow tilting vehicles. *Mathematical and Computer Modeling of Dynamic Systems* **9**, **2**, 209–231.